Surface-wave inversion for near-surface shear-wave velocity estimation at Coronation field

*Huub Douma * (ION Geophysical/GXT Imaging solutions) and Matthew Haney (Boise State University)*

SUMMARY

We study the use of surface waves to invert for a near-surface shear-wave velocity model and use this model to calculate shear-wave static corrections. We invert both group-velocity and phase-velocity measurements, each of which provide independent information on the shear-wave velocity structure. For the phase-velocity we use both slant-stacking and eikonal tomography to obtain the dispersion curves. We compare models and static solutions obtained from all different methods using field data. For the Coronation field data it appears that the phase-velocity inversion obtains a better estimate of the long-wavelength static than does the group-velocity inversion.

INTRODUCTION

In land and OBC surveys a complex near-surface can often provide a challenge in seismic data-processing. Having the ability to correct for near-surface heterogeneity in imaging can therefore be defining in the ability to successfully image the deeper lying targets. Surface waves are sensitive to a depth of roughly one wavelength. With typical observed frequencies of 3-30Hz and typical near-surface velocities, that means they carry information about the (shear-wave) velocity up to 100-150m deep. Therefore they can be used to invert for near-surface shear-wave velocity models [e.g., Xia *et al.* (1999), Ivanov *et al.* (2006), Muyzert (2007) and Gouédard *et al.* (2010)]. Such shear-wave velocity models can then be used, e.g., to calculate shear-wave static solutions.
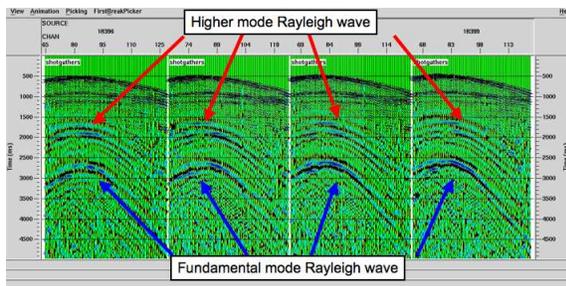

Figure 1: Observed fundamental and higher mode Rayleigh waves.

Here we compare using different measurements obtained from the surface waves to invert for the near-surface shear-wave velocity structure. We compare group-velocity and phase-velocity dispersion measurements. For the phase velocity we use both slant-stacking over a small-aperture array (van der Kruk *et al.*, 2007) and the recently developed eikonal tomography (Lin *et al.*, 2009) to obtain the dispersion curves. The inversion method used for the group and phase-velocity inversion is based on a perturbational approach applied to the forward method from Lysmer (1970) and explained in Haney & Douma (2011b).

The method is a one-dimensional finite-element method. Even though in this work we use only Rayleigh waves, the method can be extended to Love waves (Haney & Douma, 2011a). Since we are inverting dispersion curves, the inversion method is inherently one-dimensional. Hence, lateral heterogeneity is obtained by applying the method, e.g., below receiver stations. Even though the inversion is one-dimensional, the obtained models could be used as initial models for true 3D methods that can help further refine the models.

The data set we use for this work is the Coronation data set, which is a large 3D-3C data set from eastern Alberta, Canada. We show results from only one receiver line. The number of individual source-receiver pairs in this receiver line is over 100,000. The recording time for the seismic data was 6 s, ensuring that Rayleigh wave arrivals registered even at distant receivers (Figure 1). Throughout this work we use only the fundamental mode Rayleigh wave, even though the first higher mode is clearly present in the data. Using higher mode surface waves would allow to estimate the shear-wave velocity at greater depths.

GROUP VELOCITY

To obtain group-velocity dispersion curves we use Frequency-Time ANalysis (FTAN): for each source-receiver pair the traveltime related to the peak of the envelope is picked for a series of narrow bandpass filters. The resulting group delay-times can be converted to group velocity based on the offset. The obtained group-velocity is related to the average earth structure between the source and receiver. To obtain *local* dispersion curves, we apply group velocity tomography to the group-delay times along straight rays between the sources and receivers. This provides us with the group velocity $u(x,y,\omega)$. Figure 2a shows the dispersion map obtained in this way for $5Hz$. Figure 2b shows the topography of the area. We emphasize the striking correlation between the detail in the group-velocity dispersion map and the topography: in the valleys the
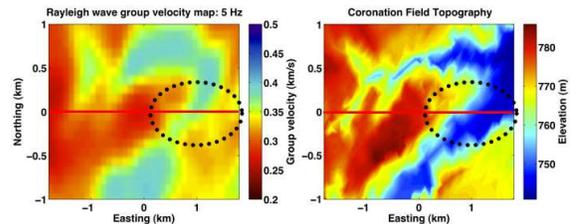

Figure 2: a) (left) group-velocity map for 5Hz and b) (right) elevation. The red line indicates the receiver locations. The heterogeneity in the group velocity map correlates very well with the topography except in the area indicated by the ellipse.

velocity is generally substantially higher (≈ 400m/s) than up

shallow (≈ 250m/s). This highlights that the velocity is increasing with depth and possibly indicates that the near surface is only mildly laterally heterogeneous. The area indicated with the dashed circle shows an area where the correlation between the velocity and the elevation is only weak, even though we know from ray-coverage plots and resolution tests that this area should be well resolved. We attribute this de-correlation to potential ray-bending effects that were ignored in the group-velocity tomography. Such ray-bending effects can, however, be included in group-velocity tomography, even though such extension is not immediately straightforward.
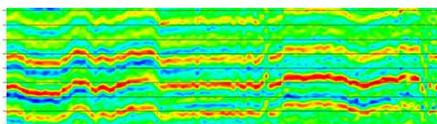

Figure 3: Raw receiver stack without any statics applied.

Once the group-velocity dispersion maps $u(x, y, \omega)$ are obtained, we can invert at each (x, y)-location the dispersion curves for a shear-wave velocity model as a function of depth. Figure 4a shows the resulting model. Using this model we can derive shear-wave statics. Figure 4 shows the near-offset receiver stack along the receiver line with shear-wave statics applied. For the purpose of comparison, Figure 3 shows the receiver stack without any statics applied. From P-wave data we know that the reflectors should be flat. Overall the group-velocity derived model provides a decent static solution, even though on the east-side we see that the static solution fails to correct for the "trough" in the reflectors. This area corresponds to the area highlighted in Figure 2 where the dispersion map does not correlate well with the topography. The remaining trough in the reflectors in this area suggests that the average velocity in the model is too high close to receiver 100. It is possible that even if ray-bending is accounted for, this area is too complex such that a 1D inversion method such as the one used here, does not produce reliable enough results.

PHASE-VELOCITY: SLANT-STACKING

To obtain phase-velocity dispersion curves, we apply slant-stacking over a small-aperture array as a function of frequency. We use the method employed by van der Kruk *et al.* (2007) but apply it here to receiver gathers with a small maximum offset of 300m (Figure 5a). An example dispersion curve is shown in Figure 5b. As opposed to the group-velocity method, no tomography is necessary, as with this method we get local dispersion curves for each receiver immediately. Therefore the dispersion curves obtained with this method contain only minor path effects as averages are taken over a small aperture only.

Comparing the static solution obtained with this method to the group-velocity method, we see that the phase-velocity method manages to better correct for the long-wavelength part of the statics, as it provides an overall slightly flatter result. However, the trough in the reflections near receiver 100 is again
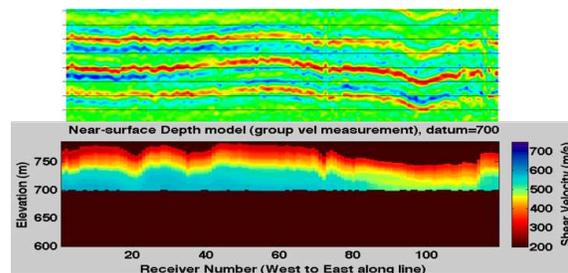

Figure 4: a) (bottom) Model derived from group-velocity dispersion curves and b) (top) receiver stack with shear-wave statics, derived from the model, applied.

present and, just like the group-velocity inversion, the phase-velocity method thus also fails to properly account for this static. Again, the overall model seems too fast in this area based on the remaining trough after the static correction.
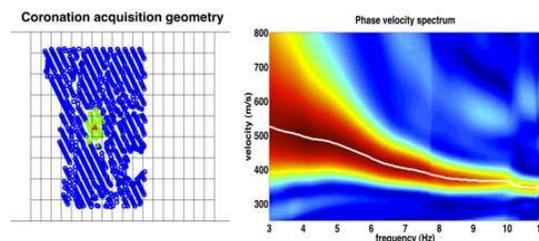

Figure 5: a) (left) Receiver (red triangle) gather used for slant-stacking. The near-offset (< 300m) sources are highlighted in green. b) (right) Phase-velocity dispersion curve.

Comparing the models obtained with the group and phase-velocity method, both models are considerably different, especially in the valley on the east side of the model (receiver number 75 to 110). This is due to the inherent non-linearity of the inversion, in combination with the fact that we used different initial models for both methods. At this stage, no particular effort was put into carefully selecting starting models for any of the methods employed in this work. Due to the non-linearity of the problem, however, careful selection of an adequate starting model can be beneficial. We shortly revisit this subject in the discusssion section. At the same time, part of the differences in the obtained models from both methods is due to the inherent different sensitivities of both methods.

EIKONAL TOMOGRAPHY

In eikonal tomography (Lin *et al.*, 2009) the traveltimes of the surface waves are picked as a function of frequency and subsequently the gradient of the traveltime maps are calculated. By the eikonal equation, this gradient equals the phase-slowness. In this way phase-velocity dispersion curves can be obtained. This method is a purely local method, as no averaging over any small aperture is used. From all methods studied in this work, eikonal tomography therefore contains the least path effects. Moreover, since many source-receiver pairs provide traveltime
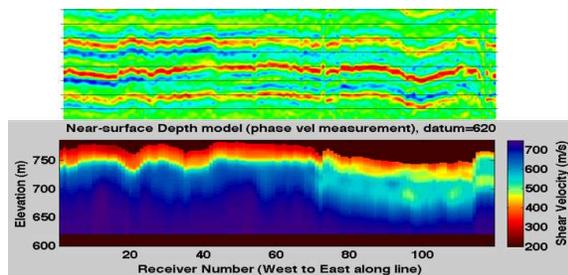
Figure 6: a) (bottom) Model derived from phase-velocity (slant-stacking) dispersion curves and b) (top) receiver stack with shear-wave statics, derived from the model, applied.

Figure 8: a) (bottom) Model derived from eikonal phase-velocity dispersion curves and b) (top) receiver stack with shear-wave statics, derived from the model, applied.

estimates, each receiver will contain many disperson-curve estimates. In this way the data variance can therefore be estimated and used in the inversion.
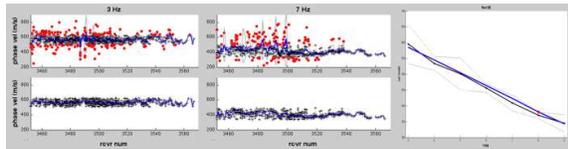

Figure 7: Phase-velocity measurements obtained from eikonal tomography at 3Hz (left) and 7Hz (middle). The red measurements are considered outliers and rejected. Right: in black the measured dispersion curve for one receiver. Error bars of one standard deviation are indicated by the grey lines.

For testing purposes we used a quick-and-dirty 2D approximation by using sources close to the receiver line only (26 sources) and approximating the gradient by taking finite differences between traveltimes from neighboring receivers. Moreover, we used only 7 frequencies ($3 - 9$Hz in equal steps of 1Hz), as opposed to both previous methods where dispersion curves were obtained at an interval of 0.05Hz, resulting in 160 different frequency measurements. Traveltimes were picked for all sources as a function of frequencies, and the resulting estimated phase-velocities are shown in Figure 7 for 3Hz and 7Hz along the whole receiver line. The red dots indicate measurements that were considered outliers due to the sources not being exactly inline with the receivers and the resulting phase velocities being calculated by simple finite differences between receiver stations. After ignoring the outliers (bottom left and middle of Figure 7) dispersion curves are obtained for all receivers. For one receiver the obtained dispersion curve is shown in the right panel of Figure 7. The error bars (i.e., data standard deviation) is indicated by the grey lines.

Using the same phase-velocity inversion as in the slant-stacking phase-velocity method, we obtain a depth model shown in Figure 8. The blue line in Figure 7 shows the predicted dispersion curve for that particular receiver. The predicted data fits the measured dispersion curve nicely for all frequencies within one standard deviation, except for the 8Hz measurement, where the predicted data is just outside the one-standard deviation range of the measurement. The shear-wave statics
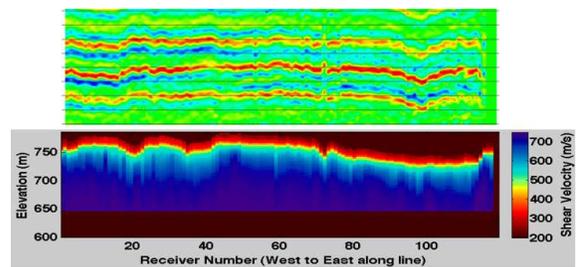
were calculated from this model and again applied to the receiver stack (top of Figure 8). The static solution is comparable with the static solution from the slant-stacking method (cf. Figure 6), even though both derived depth models are different, especially in the valley on the east-side of the receiver line. This highlights that the depth resolution for the static solution is not crucial, since only the integral measurement of the traveltime delay is needed for the static solution. Since we used a crude 2D approximation for the eikonal tomography only, with only 7 different frequency measurements, compared to the 160 frequencies used in the slant-stacking method, the lack of detail in the depth model obtained from eikonal tomography is understandable. We are currently further investigating the eikonal tomography using source-receiver reciprocity to be able to apply it in a true 3D fashion and much finer frequency sampling. We expect that this will improve the amount of subsurface heterogeneity on the east-side of the receiver line, substantially. In addition, we mention that the starting models for the slant-stacking and eikonal tomography are different, which partly explains the difference in the final models obtained. Finally, like the group-velocity and slant-stacking method, the eikonal tomography does not provide a good static solution for the trough in the reflections on the eastern side of the line close to receiver 100.

DISCUSSION

The inversion of surface waves is inherently non-linear because the sensitivity kernels depend on the model. Therefore, as is true for all non-linear methods, the inversion is dependent on the initial model. This is highlighted in figure 9, where the slant-stacking phase-velocity method was used to invert dispersion curves using two different starting models. One starting model (top left) was made based on the observation from the group-velocity dispersion map that the lower elevation correlated with higher velocities (see Figure 2), while another starting model was taken to be a fixed 1D model from the surface (top right in Figure 9). The imprint of the starting model is mostly visible in the final obtained depth models between receivers 20-45. Therefore care has to be taken in the selection of the initial model. However, we emphasize that the static solution is much less sensitive to the final obtained depth model and thus also to the initial model.

None of the methods tested provide a good static solution for the area on the eastern part of the receiver line, as is evident from the remaining "trough" in the reflections in the receiver stack. This could be related to scattering of surface waves and/or coupling problems. However, it could also well be that this particular area is too complex to warrant a 1D inversion and that full 3D methods of inversion are needed to provide a better shear-wave static solution.
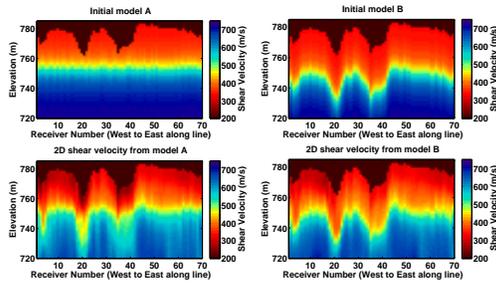

Figure 9: Comparison of models obtained using the slant-stacking-based phase-velocity method (bottom) for two different starting models (top).

At the moment we are further investigating another method that provides an independent measurement from the group-velocity and phase-velocity: the H/Z ratio, the ratio between the horizontal and vertical component of amplitude. This ratio provides an estimate of the ellipticity of the Rayleigh waves and can also be inverted for the shear-wave velocity as a function of depth (Haney *et al.*, 2011).

Even though in this work we apply surface-wave inversion to active data only, it can also be used for passive data because seismic interferometry often provides accurate estimates of the surface waves. Moreover, using interferometry, the number of source-receiver paths used in the group-velocity tomography step can be increased to provide improved ray coverage.

CONCLUSION

We have used fundamental mode Rayleigh waves to invert group-velocity and phase-velocity dispersion curves for the shear-wave velocity as a function of depth using a finite-element-based inversion method. The obtained models contain hetero-geneity on the order of 10m. Even though the inversion is non-linear and thus sensitive to the initial model, the static solution depends only on the integral of the shear-wave velocity along a ray and as such seems less sensitive to the initial model. For the Coronation data, the phase-velocity methods provide a better estimate of the long-wavelength statics than does the group-velocity method. We emphasize that the method of obtaining the shear-wave statics used here is purely based on the physics of wave-propagation, and no artificial local cross-correlation methods were used to further improve the static solution result.

EDITED REFERENCES

Note: This reference list is a copy-edited version of the reference list submitted by the author. Reference lists for the 2011 SEG Technical Program Expanded Abstracts have been copy edited so that references provided with the online metadata for each paper will achieve a high degree of linking to cited sources that appear on the Web.

REFERENCES

Gouedard, P., H. Yao, R. van der Hilst, and A. Verdel, 2010, Surface-wave Eikonal tomography in a scattering environment: Presented at the 80th Annual International Meeting, SEG.

Haney, M., and H. Douma, 2011a, Inversion of Love wave phase velocity, group velocity and shear stress ratio using finite elements: Presented at the 81st Annual International Meeting, SEG.

———, 2011b, Rayleigh wave modeling and inversion using Lysmer's method: Submitted to Geophysics.

Haney, M. M., A. Nies, T. Masterlark, S. Needy, and R. Pedersen, 2011, Interpretation of Rayleigh-wave ellipticity observed with multicomponent passive seismic interferometry at Hekla volcano, Iceland: The Leading Edge, **30**, 936–941.

Ivanov, J., R. Miller, P. Lacombe, C. Johnson, and J. Lane Jr., 2006, Delineating a shallow fault zone and dipping bedrock strata using multichannel analysis of surface waves with a land streamer: Geophysics, 71, no. 5, A39–A42.

Lin, F., M. Ritzwoller, and R. Snieder, 2009, Eikonal tomography: Surface wave tomography by phase front tracking across a regional broad-band seismic array: Geophysical Journal International, **177**, 1091–1110.

Lysmer, J., 1970, Lumped mass method for Rayleigh waves: Bulletin of the Seismological Society of America, **60**, no. 1, 89–104.

Muyzert, E., 2007, Seabed property estimation from ambient noise recordings: Part 2 — Scholte-wave spectral-ratio inversion: Geophysics, **74**, no. 4, U47–U53.

van der Kruk, J., A. Arcone, and L. Liu, 2007, Fundamental and higher mode inversion of dispersed GPR waves propagating in an ice layer: IEEE Transactions on Geoscience and Remote Sensing, **45**, 2483–2491.

Xia, J., R. Miller, and C. Park, 1999, Estimation of near-surface shear-wave velocity by inversion of Rayleigh waves: Geophysics, **64**, 691–700.